Marine Geology 311-314 (2012) 57–62

Contents lists available at SciVerse ScienceDirect

Marine Geology

journal homepage: www.elsevier.com/locate/margeo

Letter

U/Pb dating of a terminal Pliocene coral from the Indonesian Seaway

Mark C. Quigley [a,*], Brendan Duffy [a], Jon Woodhead [b], John Hellstrom [b], Louise Moody [a], Travis Horton [a], Jhony Soares [c], Lamberto Fernandes [c]

[a] Department of Geological Sciences, University of Canterbury, Christchurch 8014, New Zealand
[b] School of Earth Sciences, University of Melbourne, Victoria 3010, Australia
[c] Secretariat of State for Natural Resources (SERN), Dili, Timor-Leste

ARTICLE INFO

Article history:
Received 4 April 2011
Received in revised form 15 November 2011
Accepted 19 January 2012
Available online 28 January 2012

Communicated by G.J. de Lange

Keywords:
coral
Indonesian Throughflow
aragonite
U/Pb
Timor

ABSTRACT

Pristine detrital *Platygyra* corals were discovered in an exhumed package of syn-orogenic marine sediments on the island of Timor in the eastern Indonesian region and dated using U–Pb techniques. A single coral from the upper part of the sequence yields a $^{238}U/^{206}Pb–^{207}Pb/^{206}Pb$ concordia age of 2.66 ± 0.14 (2σ) Ma that is supported by coral $^{87}Sr/^{86}Sr$ chemostratigraphy and foraminiferal biostratigraphy from bounding strata. Minor U-series disequilibrium is best explained by U mobility within the last ~150 ka, as pore water chemistry was altered during exhumation, and is unlikely to have affected $^{238}U/^{206}Pb$ and the apparent sample age by more than 1–2%. The ability to date corals beyond the limits of ^{14}C and U/Th techniques provides the opportunity to improve the temporal resolution of associated marine chronostratigraphic records. In this instance, we refine the timing of Timor's emergence from beneath the waters of the Indonesian Seaway (*IS*) and the initiation of turbiditic deposition at the study site to between ca. 3.35 and 2.66 Ma. These results have implications for the evolution of topography and *IS* oceanic pathways in the active orogenic belts along the northern fringes of the Australian Plate.

1. Introduction

The tectonic opening and closing of oceanic pathways influence global thermohaline circulation (Berggren and Hollister, 1977), marine productivity (Schneider and Schmittner, 2006), and climate (Mudelsee and Raymo, 2005). Exhumed marine sequences in or adjacent to oceanic pathway systems (e.g., Central American seaway, Indonesian Seaway) provide opportunities to decipher tectonic, topographic, physical and chemical oceanographic pathway changes with relevance for marine faunal evolution (e.g. Jackson et al., 1996), salinity and temperature changes in adjacent oceans (e.g. Karas et al., 2009), major climate systems (e.g. von der Heydt and Dijkstra, 2011), and human evolution (Cane and Molnar, 2001). The ability to study these processes is partially limited by the difficulty in obtaining robust chronostratigraphy from marine sequences, due to factors including highly variable deposition rates, sediment reworking, lack of age-diagnostic fossils, lack of datable materials, and/or diagenetic alteration (Getty et al., 2001). U/Pb dating of detrital corals in exhumed marine sequences provides a novel and promising, albeit under-utilized, methodology to refine the chronostratigraphy of marine sequences under certain circumstances. Two prior successful attempts have been made in the Carribbean region, where U/Pb coral ages of 1.02 ± 0.07 Ma and 1.288 ± 0.034 Ma (Getty et al., 2001) and 5.52 ± 0.15 Ma (Denniston et al., 2008) were obtained. In this study, we make a first attempt to use U/Pb techniques to date pristine, detrital *Platygyra* corals from the syn-orogenic, marine Viqueque Megasequence (*VM*) presently exposed on the island of Timor in the eastern Indonesian region. Our results enable us to refine the chronostratigraphy of the *VM* and place finer temporal constraints on the onset of turbidite deposition and the emergence and vegetative colonization of the *VM* source region during a key time for *IS* evolution.

2. Geological setting

The NNE-directed voyage of the Australian continent at ~70 mm yr^{-1} relative to the Sunda Shelf (DeMets et al., 1994, see Fig. 1A) resulted in collision of the leading continental margin with the Banda Arc by the Miocene to early Pliocene (Audley-Charles, 2011; Rutherford et al., 2001). Tectonic processes including the accretion of the Banda Arc to the Australian continental crust (Bock et al., 2003; Nugroho et al., 2009) and the detachment of the downgoing slab from the Australia Plate lead to the uplift of the island of Timor (Audley-Charles, 1968; Harris, 1991; Price and Audley-Charles, 1987; Sandiford, 2008). The timing of arc-continent collision in Timor remains poorly constrained and controversial, varying from ca. 3.5 Ma (Carter et al., 1976) based on unconformities contested by Haig and McCartain (2007) to 5.5–9.8 Ma (Haig and McCartain, 2007; Keep and Haig, 2010) based on the youngest strongly deformed pre-collisional and the oldest gently deformed syn/post-collisional rocks in Timor Leste. The Timor orogen presently consists of three pre-orogenic terranes; the accreted Gondwana Megasequence and

* Corresponding author.
E-mail address: mark.quigley@canterbury.ac.nz (M.C. Quigley).

0025-3227/$ – see front matter
doi:10.1016/j.margeo.2012.01.004

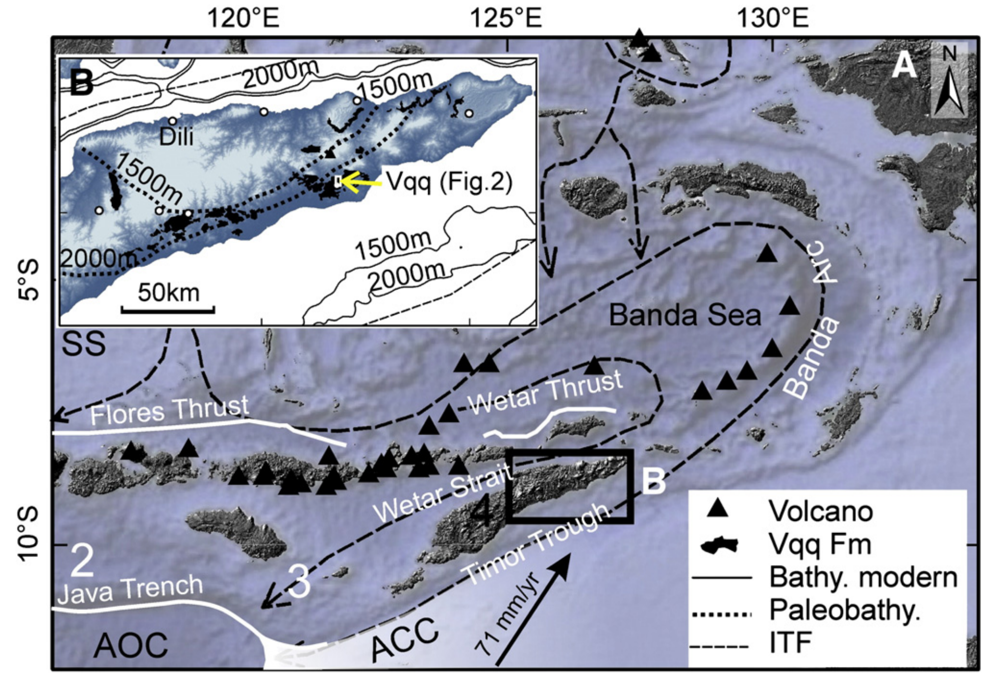

Fig. 1. (A) Timor's location relative to modern plate boundary faults (white lines and Timor Trough), Nuvel1A plate vector and the Indonesian Throughflow (Gordon and Fine, 1996). SS = Sunda Shelf; AOC = Australian Ocean Crust; ACC = Australian Continental Crust. (B) Early Pliocene paleobathymetry with correlative modern bathymetric contours.

post-Gondwana rift-drift Australian Margin Megasequences of the Australian Plate (Haig and McCartain, 2007), and the Asian-affinity Banda Terrane nappe (Harris, 2006). The latter comprises forearc basement and cover sequences that have been thrust over Australian Plate rocks. The paleo-subduction channel is expressed as an extensive mélange formation which developed between the overriding forearc and the subducting Australian plate (Harris et al., 1998; Standley and Harris, 2009). The Banda Terrane has been extensively eroded and incorporated into the *VM* (Audley-Charles, 1968; Haig and McCartain, 2007). This unit, which accumulated in extensional basins on the slope of the uplifting fold and thrust belt, has been largely eroded and is exposed primarily in the synclinal hinges of broad folds on the island (Fig. 1B).

The uplift of Timor reorganized oceanic pathways so that the proto-Timor-Sea was divided in two as parts of Timor rose from mid-bathyal depths in the terminal Miocene to terrestrial environments in the late Pliocene or early Pleistocene (Haig and McCartain, 2007; van Marle, 1991). The island is surrounded by >3000 m deep basins in both the forearc and foreland regions of the orogen (Audley-Charles, 1986; Kenyon, 1974) (Fig. 1) that serve as pathways between the Pacific and Indian Oceans that are collectively termed the *IS*. The Wetar Strait north of Timor is a young, retro-foreland basin associated with movement on the Wetar Suture that locked up around 2 Ma (Harris, 1991; Price and Audley-Charles, 1983, 1987) and foraminiferal evidence shows that the Timor Trough axis south of Timor has migrated 60–80 km south of Timor since 4.5 Ma (Veevers et al., 1978) (Fig. 1B). This migration was accompanied with the shortening and thickening of the Timor orogen, which partially blocked the *IS* and uplifted the *VM* beginning in the Early Pliocene (Keep and Haig, 2010). As such, the exhumed *VM* provides a geologic archive relevant to understanding both *IS* evolution and the uplift and erosion of its source region.

3. Stratigraphy and foraminiferal biostratigraphy of the Viqueque Megasequence

The relatively undeformed *VM* overlies structurally complex older units. The *VM* Type and Northern Cuha sections are exposed in the Cuha River on the northern limbs of WNW-striking synclines near the town of Viqueque (Fig. 2). The base of the Type section unconformably overlies the synorogenic mélange and contains mudstone clasts probably derived from the mélange matrix. The basal carbonate chalk has foraminiferal assemblages indicative of a Zone N18 age (5.2–5.6 Ma) (Batu Putih Formation; Haig and McCartain, 2007). The remainder of the Type section grades upward from pelagite to marls to a >200 m thick section of turbiditic sandstones and interbedded hemipelagic muds. The Zone N19 (4.2–5.2 Ma) marker first occurs 1.6 m above the base of the formation, the Zone N20 (3.10–4.20 Ma) marker appears at 4.9 m, and the Zone N21 (1.92–3.10 Ma) marker occurs at 34.4 m within the marl unit. The remainder of the Type section (34–240 m) belongs to Zone N21 (Haig and McCartain, 2007).

A similar stratigraphic sequence is observed in the Northern Cuha section, the base of which also belongs to Zone N18 and is stratigraphically correlative with the base of the type section. The Northern Cuha section contains several poorly sorted debris flow paraconglomerates of up to 50 m thickness (Fig. 2) that contain intact detrital corals. The corals are recorded first in the basal parts of the lowest conglomerate (Fig. 2a), intermittently within overlying conglomerates and turbidite beds, and commonly in the upper conglomerate (Fig. 2C), where they constitute ~0.1–1.0% of the total observed outcrop. Texturally,

Fig. 2. (A) stratigraphy of the Northern Cuha and Type Sections of the Viqueque Megasequence in the Cuha River, Viqueque. (B) Location of measured sections. TL07 location 8.83686°S, 126.37522°E — area location see Fig. 1B. Gray areas on map are Synorogenic Melange. (C) Vertical and lateral grainsize and thickness variation of the upper conglomerate. Note rapid transition from conglomerate into sandy turbidite with laminated woody fragments at its base. (D) Fossil tree trunk near top of the type section. (E) Insitu *Platygyra* sample, showing exceptional preservation and setting within coarse lithic dominated conglomerate.

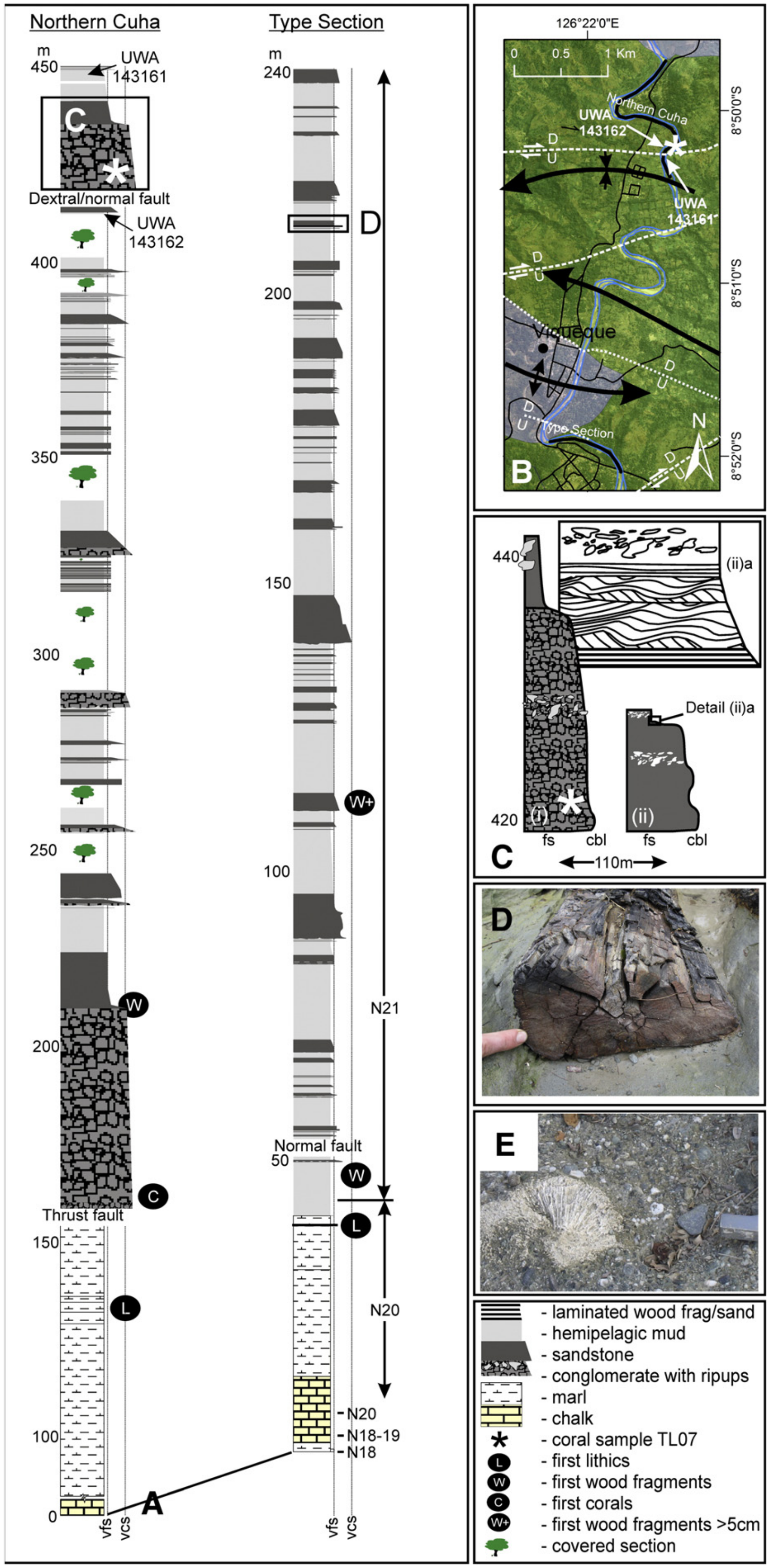
Northern Cuha
Type Section
m
450
UWA 143161
C
Dextral/normal fault
UWA 143162
400
350
300
250
200
Thrust fault
150
100
0
A
vfs
vcs
m
240
D
200
150
100
W+
N21
Normal fault
50
W
L
N20
N20
N18-19
N18
126°22'0"E
0 0.5 1 Km
Northern Cuha
UWA 143162
UWA 143161
8°50'0"S
8°51'0"S
8°52'0"S
Viqueque
Type Section
N
B
D
U
440
(ii)a
Detail (ii)a
420
(i)
(ii)
fs cbl
fs cbl
C
110m
D
E
- laminated wood frag/sand
- hemipelagic mud
- sandstone
- conglomerate with ripups
- marl
- chalk
- coral sample TL07
- first lithics
- first wood fragments
- first corals
- first wood fragments >5cm
- covered section

the upper conglomerate grades inversely from a ~10 cm thick, sandy-granular, coral-bearing basal bed to subangular, cobbly clast-supported conglomerate then alternately normally and inversely, becoming a rounded, pebbly clast-supported conglomerate before grading rapidly into sandy turbidite facies (Fig. 2C). Within this conglomerate are <25 cm diameter corals which display primary aragonitic textures with minimal observable inter-septae cements (Figs. 2e, 3D).

Foraminifera from mudstone samples UWA143159 and UWA143161, which bracket the upper conglomerate from which our sample was obtained, both belong within Zone N21 (D. Haig, *pers. comm.* 2010). Specifically, sample UWA143162, collected from a friable mudstone 1.5 m below the massive coral-bearing conglomerate bed (8.8370°S 126.3743°E), contains a planktonic foraminiferal assemblage indicative of Zone N21: *Globigerinella aequilateralis*, *Globigerinoides conglobatus*, *Gs. elongatus*, *Gs. extremus*, *Gs. immaturus*, *Gs. quadrilobatus*, *Gs. ruber*, *Gs. sacculifer*, *Gs. triloba*, dextral *Globorotalia limbata*, dextral *Gl. menardii*, *Gl. tosaensis*, sinistral *Gl. tumida*, dextral *Neogloboquadrina humerosa*, *Orbulina universa*, dextral *Pulleniatina praecursor*, and *Sphaeroidinella dehiscens* (D. Haig, *pers. comm.* 2010). Based on the species datum levels reviewed by Keep and Haig (2010), Zone N21 incorporates the 3.1 to 2 Ma interval spanning the Pliocene–Pleistocene boundary as now defined at 2.58 Ma following Gibbard et al. (2010).

The foraminiferal assemblage from UWA143162 shows evidence of dissolution associated with sedimentary pyrite formation (including infilling of some tests) in a carbonaceous mud. Planktonic foraminifera overwhelmingly dominate the preserved assemblage (>99% of recovered tests in the >150 μm sediment fraction). Among the rare benthic foraminifera are: *Cibicidoides wuellerstorfi*, *Epistomina elegans* (dominant species), *Fissurina sp.*, *Melonis pompilioides*, *Nodogenerina antillea*, *Pullenia quinqueloba*, and *Sigmoilopsis schlumbergeri* (D. Haig, *pers. comm.* 2010). This assemblage indicates that deposition probably took place in the bathyal zone at water depths between 1000 and 2000 m [based on analogy to modern species distributions from the north-eastern Indian Ocean recorded by Frerichs (1970), Peterson (1984), Van Marle (1988) and Murgese and De Deckker (2005)] (D. Haig, *pers. comm.* 2010).

In the south-dipping stratigraphic succession containing the coral locality, mudstone sample UWA143161 at 8.83762°S 126.37395°E higher in the stratigraphic succession also belongs within Zone N21 (D. Haig, *pers. comm.* 2010). The location of boundaries between N18-21 in the Northern Cuha section has not yet been obtained.

Several important events are recorded by stratigraphic marker horizons in the *VM* sections. The first appearance of turbidites occurs in the upper part of N20 at 39 m within the marl of the type section, and at 130 m in the Northern Cuha section (Fig. 2). The basal turbidite in both instances is a ~3 cm thick, thinly laminated and rippled fine-grained sand bed consisting of ~50% foraminiferal fragments and ~50% quartz and metamorphic (dominantly amphibole and chlorite) lithics likely derived from the Banda terrain to the north. The onset of turbidite deposition implies a major change in local paleogeography with the emergence of the orogenic pile above sea level and the onset of erosion.

Provenance of the turbidite and conglomerate beds in the Northern Cuha section changes up-section. Basement clasts in the lowest conglomerate are 100% mafic volcanics, schists and quartz from the Banda Terrane. Clasts in the upper conglomerate, however, although dominantly derived from the Banda Terrane (68%), also contain sandstones and mudstones (~20%) and limestone clasts that are sourced from the Gondwana Megasequence (~12%).

Woody fragments, shed off an emergent landmass, first occur as laminae within sandy turbidite beds in both the Type (50 m) and Northern Cuha (220 m) sections. In the Northern Cuha section, they occur within the sandy turbidite facies towards the top of the lowest conglomerate (Fig. 2). The grain size of the wood fragments increases up-section, as marked by the appearance of 'coarse' woody fragments (≥5 cm diameter; Fig. 2a) and even intact tree trunk segments (Fig. 2d).

The first appearance of lithics, turbidites, coastal fauna, corals, and woody detritus mark the emergence of a Timor landmass in the source region for the *VM* (Fig. 2). Biostratigraphic constraints for foraminferal assemblages bracket this between 3.35 and 1.92 Ma (Haig and McCartain, 2007). In order to better refine the minimum age of Timor emergence and vegetative colonization, we obtained a coral from the Northern Cuha section and used U/Pb dating to derive an age from this sample.

4. U/Pb dating and geochemical analysis of detrital coral

4.1. Screening

Coral sample TL07 (Fig. 2e) was extracted from the upper conglomerate, subsampled and screened for signs of diagenetic alteration following the methods of Denniston et al. (2008). X-ray diffraction (XRD) revealed 100% aragonitic composition and scanning electron microscopy (SEM) revealed a primary aragonitic skeleton with delicate growth structures, original porosity and minimal aragonitic cement and interstitial mud (Fig. 3a). Measurement of $^{234}U/^{238}U$ and

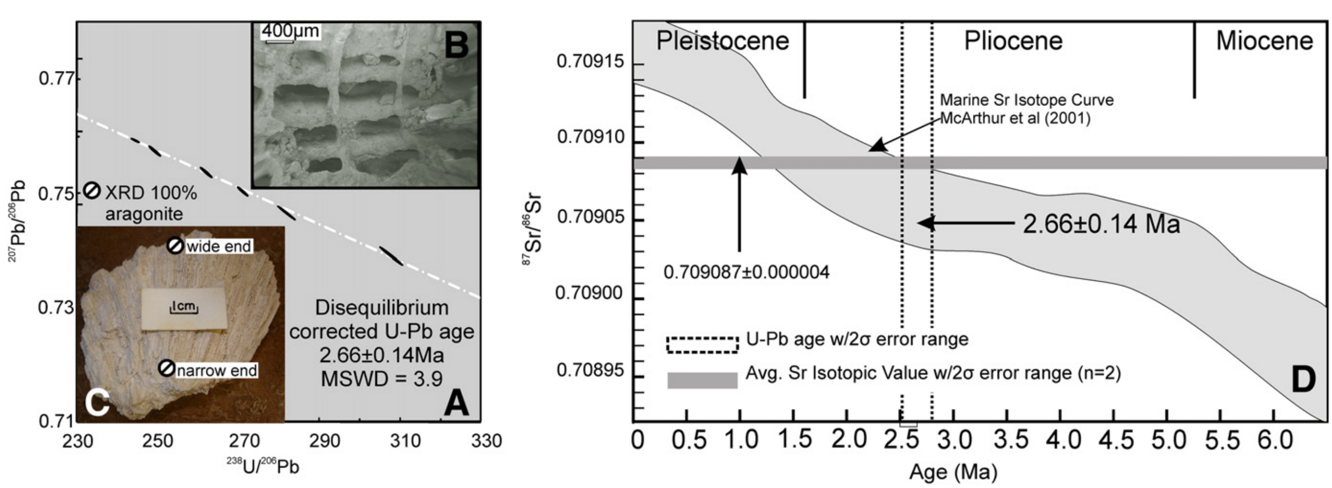

Fig. 3. (A) U/Pb isochron for TL07. (B) SEM image of well-preserved primary aragonitic coral skeleton. (C) TL07 sample indicating locations of XRD screening. (D) Marine Sr isotopic curve for the last 6.5 Ma (McArthur et al., 2001, gray area). Horizontal thick gray line represents the average Sr-isotopic ratio obtained from four *Platygyra* subsamples with 2σ error. Vertical dashed lines denote 2σ uncertainty about the U/Pb age obtained from our sample.

$^{230}Th/^{238}U$ can be a powerful diagnostic test for post-depositional mobility of U-series nuclides; where either of these ratios has departed from secular equilibrium it can be assumed that the sample has not behaved as a closed system for all of the last ~1 Ma (for ^{234}U) or ~400 ka (for ^{230}Th). Three ^{230}Th–^{234}U–^{238}U measurements were undertaken on subsamples of TL07 (Table 1) using the procedure of Hellstrom (Hellstrom, 2003), and showed minor ~2% excess ^{234}U and ~1% excess ^{230}Th.

4.2. U/Pb dating

U/Pb geochronology methods followed those outlined in Woodhead et al. (2006). Six subsamples were extracted from the coral using a dental drill, dissolved, and spiked with a mixed $^{233}U/^{205}Pb$ tracer. U and Pb were separated using conventional ion exchange techniques and isotopic ratios were measured using multicollector-inductively coupled plasma-mass spectrometery (MC-ICP-MS) at the University of Melbourne. Isotopic ratios were plotted in a $^{238}U/^{206}Pb$–$^{207}Pb/^{206}Pb$ inverse concordia ('Tera Wasserburg') plot and corrected for initial disequilibrium in the ^{238}U and ^{235}U decay chains (see Table 2 for raw data). A disequilibrium corrected age of 2.66 ± 0.14 Ma (2σ) was obtained for this sample (Fig. 3c).

4.3. $^{87}Sr/^{86}Sr$ analysis

Three further aliquots of the coral were dissolved in 3N HNO_3 and Sr was separated using Sr.Spec resin operated in nitric acid media. $^{87}Sr/^{86}Sr$ ratios were measured by MC-ICPMS, normalized to $^{86}Sr/^{88}Sr = 0.1194$ and adjusted to an SRM 987 $^{87}Sr/^{86}Sr$ value of 0.710248 as recommended by McArthur et al., 2001. An average $^{87}Sr/^{86}Sr$ value of 0.709087 ± 0.000004 (2σ) was calculated. This value intersects the upper limit of the global marine Sr curve (McArthur et al., 2001) at ~2.6 Ma (Fig. 3d). The minor discrepancy between the U/Pb and Sr-isotope ages may be attributable to a locally elevated radiogenic Sr flux due to rapid uplift and erosion of the Timor source region and/or seawater contamination that was not efficiently removed from the porous coral structure during sample processing.

5. Discussion

As demonstrated by Getty et al. (2001) and Denniston et al. (2008), the U/Pb dating of primary coral aragonite is possible providing the original coral U-series chemistry is retained and unaltered by weathering, diagenesis, and/or contaminants such as marine cement and deritus. Such preservation requires an unusual set of circumstances; the sample must have experienced little if any subaerial exposure, which would promote the calcification of aragonite, and limited burial, which would promote marine diagenesis.

Several observations suggest our calculated U/Pb age is robust; (1) the high porosity internal structure of the coral imaged by SEM indicates a general lack of alteration or contamination, (2) points on the $^{238}U/^{206}Pb$–$^{207}Pb/^{206}Pb$ concordia plot are clustered tightly to the isochron, (3) the U/Pb age is independently corroborated by foraminiferal assemblages and $^{87}Sr/^{86}Sr$ ratios, and (4) U-series analysis reveals only minor disequilibrium. The U-series disequilibrium we observe is consistent with observations of U-series nuclide behavior during diagenesis of late Pleistocene corals (Scholz and Mangini, 2007) and can be explained by post-depositional gain of U. This cannot have been sustained over the lifetime of the sample, as the heterogeneous U uptake typically observed in corals (Scholz and Mangini, 2007; Thompson and Goldstein, 2005) would then lead to more than an order of magnitude more scatter about the U/Pb isochron than we observe for TL07. The U-series disequilibrium is best explained by U mobility within the last ~150 ka as pore water chemistry altered during exhumation, and is unlikely to have affected $^{238}U/^{206}Pb$ and the apparent sample age by more than a few percent.

The lack of evidence of subaerial exposure encourages interpretation of the U/Pb age as a proxy age for the host deposit, providing that the coral was not recycled from older strata, an unlikely scenario given its fragility and age consistency with bounding strata. The co-occurrence of rounded clasts and wood fragments with the corals in the upper conglomerate suggests that the deposit was primarily derived from a near shore environment, possibly a fan delta, and not via reworking of the older sediments, although intraclasts are present at a higher stratigraphic level in the bed (Fig. 2). The U/Pb coral age provides a minimum age constraint on the first appearances of lithics, corals, and wood in the underlying strata while the lower age limit inferred from foraminiferal assemblages provides a maximum age constraint. On this basis, the time window for emergence of a proximal 'proto-Timor' source area of the *VM* from the submarine into the shallow marine and terrestrial environment is narrowed to between ca. 3.35 and 2.66 Ma. The paleobathymetry of the sediments in which our coral are encased further demonstrate that our sample was uplifted from >1000 m depth to current outcrop elevation of ~60 m *asl* since 2.66 Ma, yielding a minimum uplift rate over that period for the Viqueque Basin of ~0.4 m/ka. This is not greatly less than uplift rates of 0.6–1.6 m/ka calculated for the north coast of Timor Leste over the last 100 ka (Cox, 2009).

This is the first U/Pb age on a pre-Quaternary coral from the Indonesian region, and the first obtained Pliocene U/Pb coral age globally. The ability to date Late Cenozoic corals creates exciting opportunities for refining the chronology of marine sedimentary sequences (e.g. Denniston et al., 2008), estimating sea surface temperature and salinity conditions (e.g. Watanabe et al., 2011) and resolving the spatial and temporal evolution of their source regions. Ongoing research on corals from the *VM* aims to tie U/Pb geochronology to stable isotopic analyses to explore whether records of sea surface temperature and salinity fluctuations on monthly to yearly timescales are obtainable for deep time, including the Pliocene-to-Pleistocene transition (Moody et al., 2011).

Table 1
Platygyra raw TH/U isotope data.

$^{234}U/^{238}U$	Error (2σ%)	$^{230}Th/^{238}U$	Error (2σ%)	$^{230}Th/^{232}Th$	$^{232}Th/^{238}U$	Error (2σ%)
1.0197	0.0094	1.0067	0.0036	1092	0.002928	0.000039
1.0188	0.0042	1.0124	0.0015	41,177	0.000077	0.000002
1.0164	0.0074	1.0096	0.0017	36,960	0.000086	0.000001

All uncertainties are 95% confidence intervals and include allowances for external standard reproducibility and spike calibration uncertainty, although note that uncertainty in decay constants is not propagated.
($^{230}Th/^{238}U$) is determined using a mixed spike calibrated against a solution of HU-1 — see Hellstrom (2003) for a detailed description of the method and results of standard analyses.

Table 2
Platygyra raw U/PB isotope data.

$^{238}U/^{206}Pb$	Error (2σ%)	$^{207}Pb/^{206}Pb$	Error (2σ%)	Error correlation
244.4	0.27	0.75944	0.04	−0.824
262.0	0.45	0.75382	0.09	−0.998
281.7	0.65	0.74671	0.14	−0.999
270.9	0.37	0.75051	0.07	−0.970
249.1	0.38	0.75760	0.08	−0.991
307.7	0.72	0.73912	0.16	−0.993

All data blank corrected for 10 ± 5 pg Pb as detailed in text.

Acknowledgments

This work has profited from discussions with David Haig, Myra Keep and Eujay McCartain at the University of Western Australia and Jamie Shulmeister at University of Queensland. We thank ENI Pty Ltd, the

University of Canterbury, and the Royal Society of New Zealand Marsden Research Council (Fast-start grant M1137) for financial support. We thank the Secretariat for Energy and Natural Resources (SERN) in Dili for their continuing support for our research in Timor Leste and Joao Edmundo dos Reis, Andy Monteiro, Atino Varela and Nabe for field assistance. We thank Ron Harris, Douwe van Hinsbergen, and an anonymous reviewer for comments that improved this manuscript.

References

Audley-Charles, M.G., 1968. The Geology of Portugese Timor. Geological Society of London, London.

Audley-Charles, M.G., 1986. Rates of Neogene and Quaternary tectonic movements in the southern Banda Arc based on micropalaeontology. Journal of the Geological Society 143, 161–175.

Audley-Charles, M.G., 2011. Tectonic post-collision processes in Timor. In: Hall, R., Cottam, M.A., Wilson, M.E.J. (Eds.), The SE Asian Gateway: History and Tectonics of the Australia-Asia Collision. Geological Society Special Publications, London, pp. 241–266.

Berggren, W.A., Hollister, C.D., 1977. Plate tectonics and paleocirculation — commotion in the ocean. Tectonophysics 38, 11–48.

Bock, Y., Prawirodirdjo, L., Genrich, J.F., Stevens, C.W., McCaffrey, R., Subarya, C., Puntodewo, S.S.O., Calais, E., 2003. Crustal motion in Indonesia from Global Positioning System measurements. Journal of Geophysical Research B: Solid Earth 108.

Cane, M.A., Molnar, P., 2001. Closing of the Indonesian seaway as a precursor to east African aridification around 3–4 million years ago. Nature 411, 157–162.

Carter, D.J., Audley-Charles, M.G., Barber, A.J., 1976. Stratigraphical analysis of island arc-continental margin collision in eastern Indonesia. Journal of the Geological Society of London 132, 179–198.

Cox, N.L., 2009. Variable uplift from Quaternary folding along the northern coast of East Timor, based on U-series age determinations of coral terraces. Department of Geological Sciences. Brigham Young University, Salt Lake City, p. 151.

DeMets, C., Gordon, R.G., Argus, D.F., Stein, S., 1994. Effect of recent revisions to the geomagnetic reversal time scale on estimates of current plate motions. Geophysical Research Letters 21, 2191–2194.

Denniston, R.F., Asmerom, Y., Polyak, V.Y., McNeill, D.F., Klaus, J.S.P., Cole, P., Budd, A.F., 2008. Caribbean chronostratigraphy refined with U–Pb dating of a Miocene coral. Geology 36, 151–154.

Frerichs, W.E., 1970. Distribution and ecology of benthonic foraminifera in the sediments of the Andaman Sea. Contributions from the Cushman Foundation for Foraminiferal Research 21, 123–147.

Getty, S.R., Asmerom, Y., Quinn, T.M., Budd, A.F., 2001. Accelerated Pleistocene coral extinctions in the Caribbean Basin shown by U–Pb dating. Geology 29.

Gibbard, P.L., Head, M.J., Walker, M.J.C., 2010. Formal ratification of the Quaternary System/Period and the Pleistocene Series/Epoch with a base at 2.58 Ma. Journal of Quaternary Science 25, 96–102.

Gordon, A.L., Fine, R.A., 1996. Pathways of water between the Pacific and Indian oceans in the Indonesian seas. Nature 379, 146–149.

Haig, D.W., McCartain, E., 2007. Carbonate pelagites in the post-Gondwana succession (Cretaceous–Neogene) of East Timor. Australian Journal of Earth Sciences 54, 875–897.

Harris, R.A., 1991. Temporal distribution of strain in the active Banda orogen: a reconciliation of rival hypotheses. Journal of Southeast Asian Earth Sciences 6, 373–386.

Harris, R., 2006. Rise and fall of the Eastern Great Indonesian arc recorded by the assembly, dispersion and accretion of the Banda Terrane, Timor. Gondwana Research 10, 207–231.

Harris, R.A., Sawyer, R.K., Audley-Charles, M.G., 1998. Collisional melange development: geologic associations of active melange-forming processes with exhumed melange facies in the western Banda orogen, Indonesia. Tectonics 17, 458–479.

Hellstrom, J.C., 2003. Rapid and accurate U/Th dating using parallel ion-counting multi-collector ICP-MS. Journal of Analytical Atomic Spectrometry 18, 1346–1351.

Jackson, J.B.C., Budd, A.F., Coates, A.G., 1996. Evolution and Environment in Tropical America. University of Chicago Press, Chicago, Illinois, p. 425.

Karas, C., Nürnberg, D., Gupta, A.K., Tiedemann, R., Mohan, K., Bickert, T., 2009. Mid-Pliocene climate change amplified by a switch in Indonesian subsurface throughflow. Nature Geoscience 2, 434–438.

Keep, M., Haig, D.W., 2010. Deformation and exhumation in Timor: distinct stages of a young orogeny. Tectonophysics 483, 93–111.

Kenyon, C.S., 1974. Stratigraphy and Sedimentology of the Late Miocene to Quaternary Deposits in Timor. University of London.

McArthur, J.M., Howarth, R.J., Bailey, T.R., 2001. Strontium isotope stratigraphy: LOWESS version 3: best fit to the marine Sr-isotope curve for 0–509 Ma and accompanying look-up table for deriving numerical age. Journal of Geology 109, 155–170.

Moody, L., Quigley, M., Duffy, B., 2011. Indonesian Palaeoceanographic History Using Detrital Pliocene Corals, Geosciences 2011. Geoscience Society of New Zealand, Nelson, New Zealand.

Mudelsee, M., Raymo, M.E., 2005. Slow dynamics of the Northern Hemisphere glaciation. Paleoceanography 20.

Murgese, D.S., De Deckker, P., 2005. The distribution of deep-sea benthic foraminifera in core tops from the eastern Indian Ocean. Marine Micropaleontology 56, 25–49.

Nugroho, H., Harris, R., Lestariya, A.W., Maruf, B., 2009. Plate boundary reorganization in the active bandA arc–continent collision: insights from new GPS measurements. Tectonophysics 479, 52–65.

Peterson, L.C., 1984. Recent abyssal benthic foraminiferal biofacies of the eastern equatorial Indian Ocean. Marine Micropaleontology 8, 479–519.

Price, N.J., Audley-Charles, M.G., 1983. Plate rupture by hydraulic fracture resulting in overthrusting. Nature 306, 572–575.

Price, N.J., Audley-Charles, M.G., 1987. Tectonic collision processes after plate rupture. Tectonophysics 140, 121–129.

Rutherford, E., Burke, K., Lytwyn, J., 2001. Tectonic history of Sumba Island, Indonesia, since the Late Cretaceous and its rapid escape into the forearc in the Miocene. Journal of Asian Earth Sciences 19, 453–479.

Sandiford, M., 2008. Seismic moment release during slab rupture beneath the Banda Sea. Geophysical Journal International 174, 659–671.

Schneider, B., Schmittner, A., 2006. Simulating the impact of the Panamanian seaway closure on ocean circulation, marine productivity and nutrient cycling. Earth and Planetary Science Letters 246, 367–380.

Scholz, D., Mangini, A., 2007. How precise are U-series coral ages? Geochimica et Cosmochimica Acta 71, 1935–1948.

Standley, C.E., Harris, R., 2009. Tectonic evolution of forearc nappes of the active banda arc-continent collision: origin, age, metamorphic history and structure of the Lolotoi Complex, East Timor. Tectonophysics. doi:10.1016/j.tecto.2009.01.034.

Thompson, W., Goldstein, S., 2005. Open-system coral ages reveal persistent suborbital sea-level cycles. Science 308, 401–404.

Van Marle, L.J., 1988. Bathymetric distribution of benthic foraminifera on the Australian–Irian Jaya continental margin, Eastern Indonesia. Marine Micropaleontology 13, 97–152.

van Marle, L.J., 1991. Late Cenozoic palaeobathymetry and geohistory analysis of Central West Timor, eastern Indonesia. Marine and Petroleum Geology 8, 22–34.

Veevers, J.J., Falvey, D.A., Robins, S., 1978. Timor trough and australia: facies show topographic wave migrated 80 km during the past 3 m.y. Tectonophysics 45, 217–227.

von der Heydt, A.S., Dijkstra, H.A., 2011. The Impact of Ocean Gateways on ENSO Variability in the Miocene. , pp. 305–318.

Watanabe, T., Suzuki, A., Minobe, S., Kawashima, T., Kameo, K., Minoshima, K., Aguilar, Y.M., Wani, R., Kawahata, H., Sowa, K., Nagai, T., Kase, T., 2011. Permanent El Niño during the Pliocene warm period not supported by coral evidence. Nature 471, 209–211.

Woodhead, J.D., Hellstrom, J., Maas, R., Drysdale, R., Zanchetta, G., Devine, P., Taylor, E., 2006. U–Pb geochronology of speleothems by MC-ICPMS. Quaternary Geochronology 1, 208–221.